

Buoyancy Effects on Forced Convection from a Horizontal Cylinder in a Crossflow

R. A. Ahmad*

Thiokol Corporation/Space Operations, Brigham City, Utah 84302
and

Z. H. Qureshi†

Westinghouse Savannah River Company, Aiken, South Carolina 29803

An experimental investigation of buoyancy effects on forced convection heat transfer from a horizontal cylinder dissipating a uniform heat flux was conducted. An open-loop wind tunnel was used to provide crossflow over the cylinder. The heat flux for the 4.45-cm-diam, 38-cm-long cylinder was varied between 10–250 W, and the flow velocities were varied from 1.4 to 8 m/s. This resulted in Reynolds number and modified Grashof number values in the ranges of 3.2×10^3 to 2.13×10^4 , and 2.8×10^6 to 5.7×10^7 , respectively. The local Nusselt number is correlated as a function of the Reynolds and modified Grashof numbers. The average Nusselt numbers from the present results in the forced and mixed convection regimes are also correlated. These correlations are also compared with the available correlations in literature.

Nomenclature

A	= cylinder outer surface area, m^2
D	= cylinder diameter, m
dA_i	= surface area of individual element on cylinder, m^2
Gr_D	= Grashof number based on outer diameter, $g\beta(T_s - T_\infty)D^3/\nu^2$
Gr_D^*	= modified Grashof number based on outer diameter, $g\beta q'' D^4/(k\nu^2)$
g	= acceleration due to gravity, m/s^2
h	= local heat transfer coefficient, $W/m^2 K$
k	= thermal conductivity of air, $W/m K$
Nu_D	= Nusselt number based on outer diameter, hD/k
n	= exponent in the buoyancy parameter
Pr	= Prandtl number, ν/α
q	= heat transfer rate, W
q''	= heat flux (q/A), W/m^2
$R_{c,hot}$	= total hot resistance of cylinder wires and wire connections, Ω
Ra_D	= Rayleigh number based on outer diameter, $Gr_D Pr$
Ra_D^*	= modified Rayleigh number based on outer diameter, $Gr_D^* Pr$
Re_D	= Reynolds number based on outer diameter, $U_\infty D/\nu$
T	= temperature, K
T_m	= arithmetic mean temperature, $(\bar{T}_s + T_\infty)/2$, K
Tu	= calculated or measured freestream turbulence intensity, %
U	= mean velocity, m/s
V	= bridge voltage, V
α	= thermal diffusivity of air, m^2/s
β	= coefficient of volumetric expansion of air, $1/T_\infty$, K^{-1}

ε	= emissivity of the cylinder outer surface
θ	= angular coordinate, deg, shown in Fig. 2
θ_B	= $270 - \theta$, deg, Fig. 5
κ	= mixed convection parameter based on Grashof number, $Gr_D/(Re_D)^2$
κ^*	= mixed convection parameter based on modified Grashof number, $Gr_D^*/(Re_D)^{1.8}$
μ	= dynamic viscosity of air, $N\cdot s/m^2$
ν	= kinematic viscosity of air, μ/ρ , m^2/s
ρ	= density of air, kg/m^3
σ	= Stefan-Boltzmann constant, $5.669 \times 10^{-8} W/m^2 K^4$

Subscripts

c	= convective, drop across cylinder
D	= cylinder outer diameter
f	= forced convection, $\kappa \approx 0$, $\kappa^* \approx 0$
i	= individual element of cylinder
r	= radiative
s	= at surface
t	= total
∞	= freestream conditions

Superscripts

$\bar{}$	= average
''	= flux

Introduction

THE objective of this study was to investigate buoyancy effects on forced convection from a horizontal cylinder dissipating a uniform heat flux to a crossflow stream of air. This experimental study was undertaken to cover a range of Reynolds (Re_D) and modified Grashof numbers (Gr_D^*) by varying the flow velocities and surface heat flux values. The term “free” or “natural” will be used interchangeably to represent pure buoyancy induced flow. The term “combined” or “mixed” convection represents the conditions where both free and forced convection mechanisms are present. This region is commonly characterized by $Gr_D^*/(Re_D)^n$, the mixed convection parameter. The following information was specifically sought: 1) variation of local Nusselt number around the cylinder with the modified Grashof and Reynolds numbers; 2) variation of the average forced convection Nusselt number with the Reynolds number; 3) variation of average mixed

Presented as Paper 92-0711 at the AIAA 30th Aerospace Sciences Meeting, Reno, NV, Jan. 6–9, 1992; received June 18, 1992; revision received Dec. 22, 1992; accepted for publication Dec. 22, 1992. Copyright © 1992 by the American Institute of Aeronautics and Astronautics, Inc. All rights reserved.

*Scientist and Member of the Technical Staff, Engineering Analysis Department, M/S L63, P.O. Box 707. Senior Member AIAA.

†Manager, New Production Reactor (NPR) Thermal Hydraulics, 1995 S. Centennial Ave., CCC Bldg. 4.

convection Nusselt number with the mixed convection parameter; and 4) determination of a parameter which defines the boundary between the forced and mixed convection regimes.

Most past research in the area of convective heat transfer has focused on either pure forced or pure natural convection regimes. At high Reynolds numbers, the heat transfer occurs mainly by forced convection, but as the Reynolds number decreases, the contribution of natural convection becomes significant. In any convective heat transfer, temperature differences occur in the boundary region near the heated surface. These differences cause density gradients in the ambient medium, and in the presence of a body force field, e.g., gravity, natural convection effects result.

From a practical standpoint, the extent of these natural convection effects, and when they may be neglected, as compared to forced convection effects, must be determined. In many situations these two effects are of comparable order, such as in the use of hot-wire/film anemometry in low-velocity fields, in natural convection in the presence of ambient fluid circulations, in low-flow heat exchangers where strong temperature gradients may exist, and in cooling of electronic devices.

Analysis indicates the parameter which characterizes mixed convection is a combination of Grashof number and Reynolds number $Gr_D/(Re_D)^n$. The limits $Gr_D/(Re_D)^n \rightarrow 0$ and $Gr_D/(Re_D)^n \rightarrow \infty$ correspond to forced and natural convection regimes, respectively. The exponent " n " has the value between 2 and 3, depending on the geometry and the thermal boundary conditions. Since the distinction between the pure natural and the pure forced convection regimes is gradual, arbitrary criteria may be established to identify the three transport regimes, 1) natural, 2) mixed, and 3) forced convection.

Previous Work

Mixed convection processes may be considered in terms of external flow over surfaces, in terms of free boundary flow (e.g., plumes and buoyant jets), and in terms of internal flow in tubes, channels, and enclosed flow regions. Only the literature on external flow over cylindrical geometries is discussed here.

Van Der Hegge Zijnen¹ made the first attempt at combining the natural and forced convection effects vectorially. This approach is difficult to justify on physical grounds since Nusselt numbers are not vectors. Based upon an experimental study using air, Collis and Williams² recommended that natural convection contribution is negligible when $Re_D > (Gr_D)^{1/3}$. Sparrow and Lee³ and Joshi and Sukhatme⁴ presented analytical solutions for aiding mixed convection flows. Merkin⁵ extended the study of Sparrow and Lee³ for large Reynolds and Grashof numbers for hot and cold cylinders using the boundary-layer equations. Jain and Lohar⁶ considered the flow of a uniform stream over a horizontal circular cylinder in the case of an aiding flow. Nakai and Okazaki⁷ analyzed aiding, opposing and crossflow mixed convection when either forced or free convection is dominant. Badr⁸ presented a numerical solution of full Navier-Stokes equations representing mixed convection heat transfer from an isothermal circular cylinder in crossflow.

Numerous experimental studies on mixed convection from a horizontal circular cylinder are reported in the literature. Hatton et al.⁹ investigated combined convection from a horizontal cylinder for the Reynolds and Rayleigh number ranges of $10^{-2} \leq Re_D \leq 45$ and $10^{-3} \leq Ra_D (= Gr_D Pr) \leq 10$. The effect of freestream direction on the heat transfer process was also investigated. Oosthuizen and Madan¹⁰ correlated their test data on aiding mixed convection from an isothermal cylinder as

$$\overline{Nu}_D/\overline{Nu}_{D,f} = 1.0 + 0.18\kappa - 0.011(\kappa)^2 \quad (1a)$$

where the forced convection Nusselt number is given by

$$\overline{Nu}_{D,f} = 0.464(Re_D)^{0.5} + 0.0004Re_D \quad (1b)$$

for $100 \leq Re_D \leq 3162$, $3.75 \times 10^4 \leq Gr_D \leq 3.00 \times 10^5$, and $0 \leq [\kappa = Gr_D/(Re_D)^2] \leq 9$. They also found forced convection to exist when $\kappa < 0.28$. Based upon the same data, Jackson and Yen¹¹ suggested an improved correlation. Oosthuizen and Madan¹² in a later study suggested values for κ below which the buoyancy effects may be neglected under aiding, opposing, and crossflow conditions. They found that under aiding and crossflow conditions, the buoyancy forces increased the heat transfer rate beyond the forced convection rates. They also found that for opposing flows, the buoyancy forces decrease the Nusselt number at low Reynolds numbers and then rise above the forced flow values at high Reynolds numbers. The initial decrease in mixed convection Nusselt number is also reported in Refs. 8, 9, and 13 for low Reynolds number. Other experimental studies include those in Refs. 14–19. Morgan²⁰ provided an extensive review on convective heat transfer from a horizontal cylinder and suggested several correlations.

Baughn²¹ investigated the effect of the circumferential wall heat conduction (which occurs as a result of the circumferential temperature variation) on wall heat flux boundary condition, and concluded that it can be minimized by selection of low thermal conductivity material, a thin wall, or a large diameter. A large-diameter cylinder requires a large test section (to minimize blockage effect) which requires a large wind tunnel. The wind-tunnel dimensions must be compatible with the available laboratory space. Seban²² and Giedt²³ used a Nichrome ribbon attached to a plastic substrate. Petrie and Simpson²⁴ used a thin, stainless-steel foil rolled into a cylindrical shape and filled with epoxy resin. In the limit, the thin electrical heating element on the surface can be reduced to a coating applied to the surface. Hatton and Woolley²⁵ used a plastic substrate with a copper coating in a flat duct. Simonich and Moffat²⁶ and Hippensteele et al.²⁷ used a gold-coated plastic sheet as the heating element in conjunction with liquid crystals for thermal visualization of heat transfer. Baughn et al.^{28,29} developed a technique which involves using a thin gold coating vacuum deposited on a pliable polyester sheet as the electrical heating element. The sheet was glued to the inner surface of a thin-walled, cast acrylic tube.

Experimental Apparatus and Procedure

The experimental apparatus in the present study consisted of a low-speed open-loop wind tunnel (Fig. 1), a test cylinder, and the associated instrumentation. Details of the wind tunnel are given in Refs. 30 and 31. As shown in Fig. 1, the test section has a 38 by 38 cm cross section, with a length of 38 cm. The test section was made of clear Plexiglas® for easy viewing.

Downstream of the test section is a three-dimensional, manually controlled traversing mechanism. Temperature and velocity probes can be moved manually in all three dimensions with a 0.127-mm resolution. To minimize the blockage effect, the traversing mechanism is controlled from the outside. The traversing mechanism section is followed by a smooth divergent duct, the diffuser. A variable-speed, vane-axial fan was used at the diffuser outlet to provide air velocities of 1.4–9.1 m/s. Although the wind tunnel can provide flow in any arbitrary direction, it was used only in a horizontal position for this study. The average velocity in the test section was measured by a pitot tube. An inclined manometer, with a minor-scale division of 0.127 mm of water, was used to measure the pressure differential. This yielded a velocity resolution of 0.16 m/s. The uncertainty associated with velocity measurements was 11% for the minimum velocity (1.4 m/s) and 2% for the maximum velocity (8 m/s). The wall boundary layer was found to be less than 2.54-mm thick. A Danske Industry Syndicate

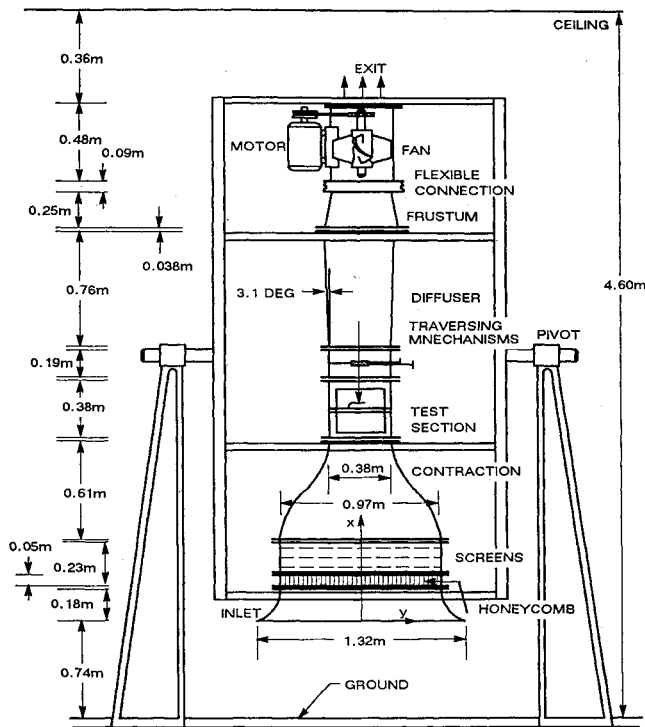


Fig. 1 Wind-tunnel schematic.

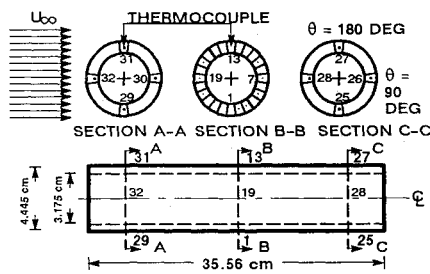


Fig. 2 Details of the test cylinder.

A/S (DISA) hot-wire anemometer system in the constant temperature mode was used to measure the mean velocity and the freestream turbulence intensity in the test section. With the screens present, the turbulence intensity was measured at 0.25% at 9.1 m/s. The test cylinder was fabricated from a 3.175-cm i.d., 4.445-cm o.d., and 38.10-cm-long hard fiber tube (Fig. 2) of low-thermal conductivity material (0.29 W/m-C). The test cylinder blocked 11.67% of the test section. The heat flux for the test cylinder was varied between 10–250 W, and the flow velocities were varied from 1.4 to 8 m/s, giving a maximum heat flux of 5000 W/m². Twenty-four V-shaped grooves of 35.56 cm in length were machined around the circumference to accommodate 24 Nichrome heaters. This left 1.27 cm of unheated length on each end of the cylinder to reduce end losses. Insulating end caps were added to reduce further end losses. The grooves were filled with copper oxide cement, which has good thermal and poor electrical conductance. At the middle of the cylinder length, 24 thermocouples were buried in the copper oxide cement, approximately 0.254-mm below the surface. Four more thermocouples were placed, 90-deg apart, at another axial location to check the two-dimensionality of the test cylinder. They were found to agree with the corresponding thermocouples located at the middle of the cylinder length.

The 0.508-mm separation (hard fiber material) between two adjacent grooves on the cylinder surface and the 5.08-mm separation at the groove depth were determined to be sufficient to minimize the circumferential heat conduction for non-

isothermal boundary conditions. The cylinder surface was machined and polished. To minimize the radiation losses, which are commonly present in air, a thin film of aluminum was deposited on the cylinder surface by the vacuum metallization process. Since each heater can be heated independently, any thermal boundary condition may be achieved on the cylinder surface. In this study, all the heaters were connected in series to yield a uniform heat flux thermal boundary condition.

The thermocouple lead wires were connected to the terminals of a selector switch. Temperatures were measured, with 0.25°C resolution from the chromel-alumel thermocouple signals recorded on a two-channel chart recorder.

The test cylinder was heated by a Hewlett Packard precision-regulated power supply to give a steady uniform heat flux boundary condition on the cylinder surface. The heat flux was computed by the voltage drop across the cylinder and the total hot resistance of the heaters. In each run, a steady-state temperature distribution over the entire circumference of the cylinder was obtained for a given value of heat flux and average velocity. Thermophysical properties were evaluated at the arithmetic mean of the average surface temperature of the cylinder and that of the ambient air, except the coefficient of the volumetric expansion (β), which was taken at the ambient temperature.

The contribution of the radiative heat transfer from each element was calculated as follows:

$$q_{r,i} = \sigma \epsilon [(T_{s,i})^4 - (T_\infty)^4] dA_i \quad (2)$$

where the emissivity (ϵ) was estimated to be 0.10. The heat loss by convection ($q_{c,i}$) from an element was computed by subtracting the radiation loss ($q_{r,i}$) from the total heat input (electric power) to that element (q_i).

$$q_{c,i} = q_i - q_{r,i} \quad (3a)$$

Local values of the Nusselt number were calculated as follows:

$$Nu_{D,i} = h_i \frac{D}{k} = \frac{\{[V^2/(R_{e,hot})/24] - q_{r,i}\}}{(T_{s,i} - T_\infty) dA_i} \left(\frac{D}{k}\right) \quad (3b)$$

The average Nusselt number was obtained by numerically integrating the 24 local values of local Nusselt numbers. It is defined as

$$\overline{Nu}_D = \frac{1}{2\pi} \int_0^{2\pi} Nu_{D,i} d\theta \quad (3c)$$

Experimental Results and Discussion

This section describes the experimental results of forced and mixed flow obtained in this study. The following results are discussed here: 1) local Nusselt number profiles, 2) averaged Nusselt number, and 3) boundary between forced and mixed flow regimes.

A total of 172 runs were made by varying the heat flux and velocity. Figure 3 shows each experimental run with the corresponding independent and dimensionless Reynolds and modified Grashof numbers. This figure provides a quick look at the region where the experiments were conducted. The dimensionless parameters in the present study were varied as follows: $3.28 \times 10^3 \leq Re_D \leq 2.13 \times 10^4$, $2.80 \times 10^6 \leq Gr_D^* \leq 5.66 \times 10^7$, and $0.24 \leq \kappa^* \leq 4.8$.

Local Nusselt Number Profiles

As presented in Fig. 3, a wide range of Reynolds and modified Grashof number conditions were achieved. In order to systematically determine the buoyancy effects on forced convection, the local Nusselt number profiles are presented here at selected values of Reynolds numbers. For each selected Reynolds number, several profiles presented for increasing modified Grashof number.

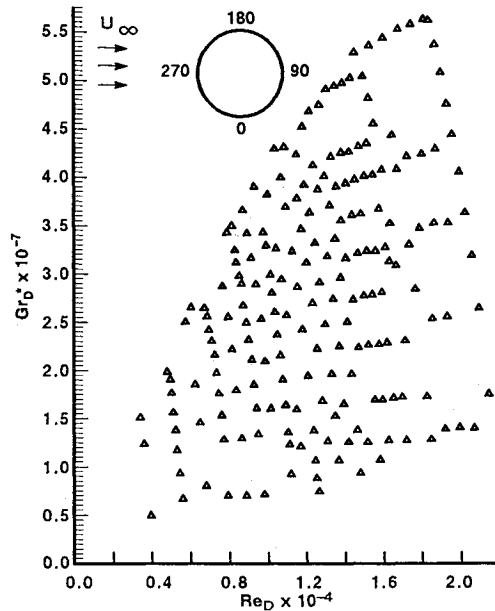


Fig. 3 Experimental runs corresponding to modified Grashof and Reynolds numbers.

Figure 4a shows the local Nusselt number to be symmetrical for $Re_D = 0.5 \times 10^4$ and small buoyancy effects represented with $Gr_D^* = 0.5036 \times 10^7$. As the Grashof number increases, the local Nusselt number increases at every angular location and some distortion of the symmetry starts to appear.

Consider the curve showing the local Nusselt number for the combination of $Re_D = 0.5 \times 10^4$ and $Gr_D^* = 0.5036 \times 10^7$ shown in Fig. 4a. Then in considering the upper half of the cylinder, starting at the forward stagnation point ($\theta = 270$ deg), $Nu_D(\theta)$ decreases with decreasing θ due to laminar boundary-layer development, and a minimum ($Nu_D = 19.13$) is reached at $\theta \approx 150$ deg. At this point, separation occurs and $Nu_D(\theta)$ increases slightly with decreasing θ due to mixing associated with vortex formation in the wake. The next three curves (for higher values of Gr_D^*) show more increase in the value of $Nu_D(\theta)$ with decreasing θ from the forward stagnation point (due to more mixing), and the separation point moves gradually clockwise to about $135 \leq \theta$ (deg) ≤ 150 deg. At the forward stagnation point ($\theta = 270$ deg), the local Nusselt number increased from 36.9 for $Gr_D^* = 0.5036 \times 10^7$ to 53 for $Gr_D^* = 2.4884 \times 10^7$, resulting in an increase of about 42%.

The effect of buoyancy on the local Nusselt number at the forward ($\theta = 270$ deg) and rear ($\theta = 90$ deg) stagnation points and their relative magnitudes are investigated. Figures 4b–d show a similar behavior to that shown in Fig. 4a, more noticeable distortion of the forced convection Nusselt number profile. In Fig. 4b, for $Gr_D^* = 4.6968 \times 10^7$, the local Nusselt number at the angular location of $\theta = 270$ deg (89) is higher than the local Nusselt number at the angular location of $\theta = 90$ deg (78) by as much as 14%. In Figs. 4c and 4d, the difference in the maximum local Nusselt at the angular locations of $\theta = 270$ deg and $\theta = 90$ deg is about 5 and 3%, respectively.

Figures 4a–d show clearly that the local Nusselt number has increased with the buoyancy effects at every angular location on the cylinder surface. The forced convection Nusselt number profiles have been distorted.

Figure 5 shows two comparisons between our results at $Re_D = 3275$ and $17,935$ (with buoyancy effects) and the results of other studies based on the local Nusselt number. All of these studies used a uniform heat flux thermal boundary condition.

The first was made between our results at $Re_D = 3275$ and $Gr_D^* = 1.5209 \times 10^7$ (Fig. 5a) and the results of Sarma and

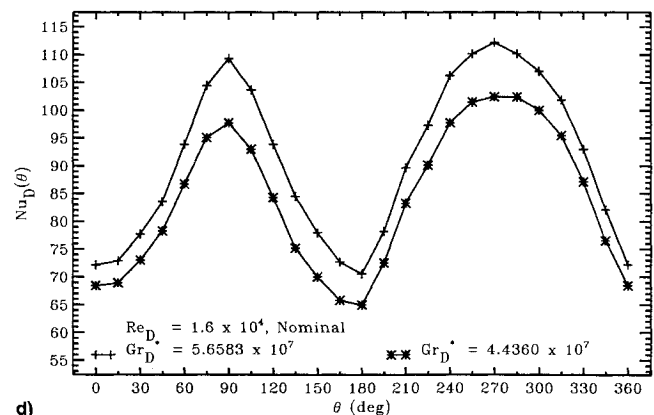
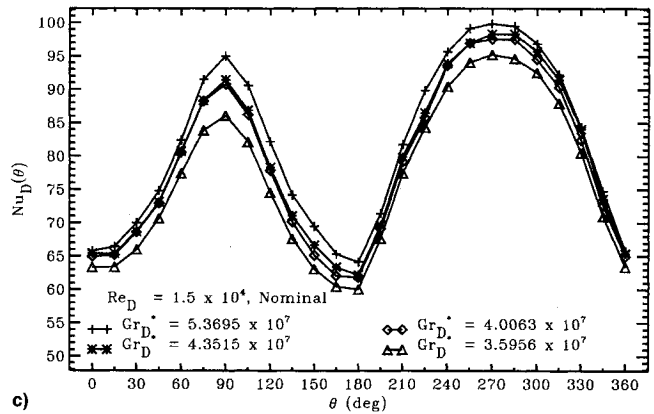
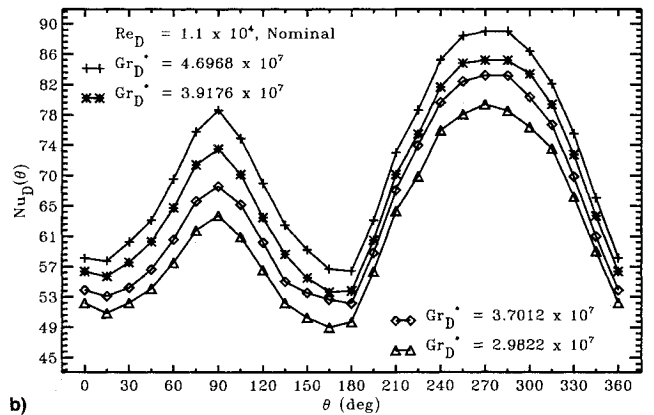
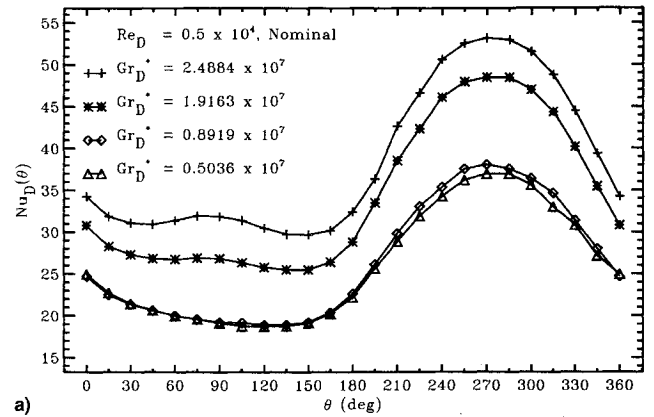


Fig. 4 Distribution of local Nusselt number around the cylinder as a function of Reynolds and modified Grashof numbers; $Pr = 0.7$. Buoyancy effects on $Re_D =$ a) 0.5×10^4 , b) 1.1×10^4 , c) 1.5×10^4 , and d) 1.6×10^4 .

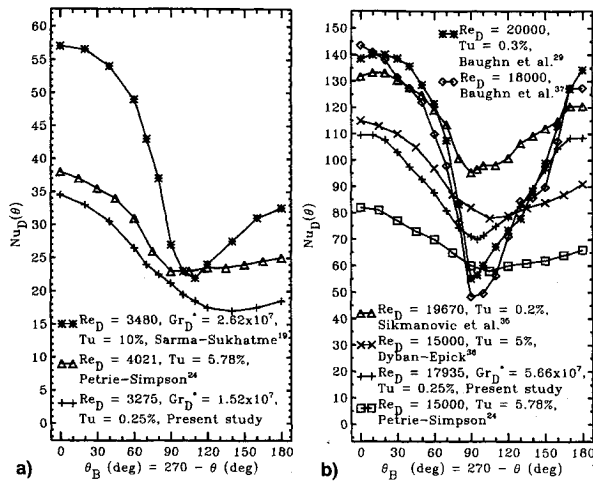


Fig. 5 Nusselt number distribution for single cylinder with uniform heat flux thermal boundary condition; $Pr = 0.7$.

Sukhatme¹⁹ in forced convection with buoyancy effects at $Re_D = 3480$ and $Gr_D^* = 2.62 \times 10^7$. Using their definition of the buoyancy parameter as $Gr_D^*/(Re_D)^{2.5}$, the above values of Re_D and Gr_D^* result in values of this parameter of 0.025 (present study) and 0.037 (Sarma and Sukhatme¹⁹), respectively. Clearly, the results of Sarma and Sukhatme¹⁹ and the results of Petrie and Simpson²⁴ show higher values for the local Nusselt number than our results, especially at the forward side of the cylinder. We attribute their larger values to the higher free-stream turbulence intensity ($Tu = 10$ and 5.78% , respectively) in their wind tunnels, whereas in our tunnel, it was 0.25% . At the forward stagnation point ($\theta_B = 0$ deg), their values of the local Nusselt numbers are larger than the present value by 65.22 and 10.14% , respectively. Kestin³² demonstrated the local effect of freestream turbulence intensity on the rate of heat transfer and, therefore, on the characteristics of the associated laminar boundary layer [$0 \leq \theta_B$ (deg) ≤ 60]. The effect was unexpectedly large,³² reaching a value of 80% at the forward stagnation point for a change of freestream turbulence intensity from 0% (calculated by Frossling³³) to less than 3% (measured). The local measurements of Nusselt number conducted by Lowery and Vachon³⁴ showed that in the laminar boundary layer, small increases in freestream turbulence intensity between 0.4 – 1.2% markedly increased the local rate of heat transfer. Increases in heat transfer over the theoretical zero freestream turbulence intensity value were on the order of 20% . Increases in heat transfer over the zero freestream turbulence intensity value ($Tu = 0$) up to approximately 60% were obtained at the highest values of freestream turbulence intensity of 14.19% . The data of Petrie and Simpson²⁴ demonstrated the sensitivity of heat transfer to freestream turbulence intensity in the wake region [$90 \leq \theta_B$ (deg) ≤ 180]. In the Reynolds number range of 5000 – $35,000$, increases in freestream turbulence intensity of 10% result in improvements on heat transfer up to 100% . They obtained an expression for the local Nusselt number at the rear stagnation point ($\theta_B = 180$ deg) as

$$Nu_D = 0.0065(Re_D)^{0.89} + [1 + 6.3 \times 10^3(Tu/Re_D)^{0.74}]^{1.1} \quad (4a)$$

which reduces to

$$Nu_D = 0.0065(Re_D)^{0.89} \quad (4b)$$

when there is zero freestream turbulence intensity. Sikmanovic et al.³⁵ found that the greatest increase of the local Nusselt number occurs in the laminar boundary layer. They also demonstrated that for $Tu = 14\%$, the Nusselt number shows two minima.

The second comparison was made between our results at $Re_D = 17,935$ and $Gr_D^* = 5.6583 \times 10^7$ (Fig. 5b) and the results of Baughn et al.²⁸ at $Re_D = 20,000$ ($Tu = 0.3\%$), Sikmanovic et al.³⁵ at $Re_D = 19,670$ ($Tu = 0.2\%$), Petrie and Simpson²⁴ at $Re_D = 15,000$ ($Tu = 5.78\%$), Dyban and Epick³⁶ at $Re_D = 15,000$ ($Tu = 5\%$), and Baughn et al.³⁷ at $Re_D = 18,000$ ($Tu = \text{unknown}$). The divergence of the results in the laminar boundary layer is attributed to the freestream turbulence intensity. In all these studies, it was desired to operate a low-turbulence, low-blockage tunnel, and to make accurate measurements. The divergence of the results beyond the laminar boundary layer and in the rear of the cylinder may be attributed to numerous factors: 1) different values of the Reynolds number ($15,000 \leq Re_D \leq 20,000$ as shown in Fig. 5b); 2) tunnel geometries which include interplay of the type and size of the test section, blockage, aspect ratio, and wall effects; 3) the freestream turbulence intensity has also an effect in the wake region;²⁴ 4) the uniform heat flux boundary condition achieved by Baughn et al.²⁸ was better than other studies shown in Fig. 5b, since their design minimized the circumferential wall conduction; 5) the emissivity of the outer surface increases as the surface degrades—this effect reduces the convection term as shown in Eq. (3a); and 6) cylinder diameter is likely to have some effect via the integral length scale of turbulence, as demonstrated by Van Der Hegge Zijnen.³⁸ Achenbach³⁹ claims that the occurrence of small differences in the flow conditions when using two different test cylinders in the same facility could not be ruled out.

Averaged Nusselt Number

The average Nusselt number in the forced convection regime ($\kappa^* = 0$), based on the present results, is best correlated (using the least-squares method) as

$$\overline{Nu}_{D,f} = 0.0675(Re_D)^{0.7333}, \quad 6.8 \times 10^3 \leq Re_D \leq 2.13 \times 10^4 \quad (5)$$

The condition for forced convection ($\kappa^* \approx 0$) was achieved when the Nusselt number ratio was in the range $1.0 \leq \overline{Nu}_D/\overline{Nu}_{D,f} < 1.05$. No data was shown for $\kappa^* < 0.2$.

Morgan²⁰ analyzed the results of 13 workers who gave the freestream turbulence intensity in the wind tunnel they used. In all these studies, a uniform wall-temperature boundary condition²⁰ was used, with the exception of the study conducted by Krall and Eckert¹⁸ ($5 \leq Re_D \leq 5000$) where a uniform heat flux boundary condition was used. At the Reynolds number 2×10^4 , the measured Nusselt number varied from 65 to 119 , with a mean value of 100.8 and a standard deviation of 12.3 . In the present study, the measured Nusselt number at $Re_D = 2 \times 10^4$ was 96.22 , which is 3.93 less than the mean value reported. After Morgan's²⁰ correction for blockage and freestream turbulence intensity errors, the range becomes 68 – 93 , the mean 79.9 , and the standard deviation 7.2 . Based on these studies, Morgan proposed the following correlation:

$$\overline{Nu}_{D,f} = 0.148(Re_D)^{0.633}$$

for

$$5 \times 10^3 \leq Re_D \leq 5 \times 10^4 \quad (6)$$

Our correlation [Eq. (5)], together with the Morgan's correlation²⁰ are plotted in Fig. 6. The forced convection Nusselt number obtained from the present study is higher than the Nusselt number obtained by Morgan as Reynolds number increases in the range shown. The difference is attributed to different thermal boundary conditions. This is in agreement with other numerical results in Refs. 13 and 40, that the uniform heat flux horizontal cylinder has a higher averaged Nusselt number than a cylinder under a uniform surface temperature. This is also true for forced convection on a flat plate⁴¹ and natural convection on a vertical plate.⁴²

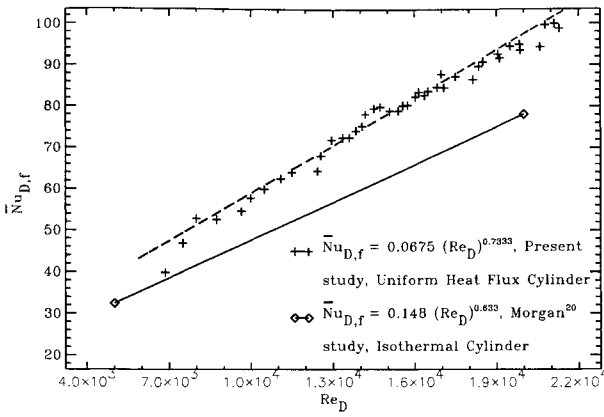


Fig. 6 Average Nusselt number in forced convection.

The results of uniform heat flux measurements conducted by Baughn and Saniei,⁴³ Papell,⁴⁴ and O'Brien et al.⁴⁵ were directly compared to those of uniform surface temperature. The Nusselt number at the forward stagnation point⁴³ was found to be nearly identical for both thermal boundary conditions. As the laminar boundary layer builds up on the front of the cylinder, the Nusselt number for the uniform heat flux is higher than that for the uniform surface temperature. Similar behavior was observed by both Papell⁴⁴ and O'Brien et al.⁴⁵ Papell⁴⁴ obtained local Nusselt number over the leading surface of a cylinder in crossflow for $50,000 \leq Re_D \leq 215,000$. The local Nusselt numbers for angular distance between 60–80 deg at the front side of the cylinder are in disagreement with other studies. The absolute values of the Nusselt number were not of primary interest, but rather the accuracy of the relative differences between the uniform heat flux and uniform surface temperature thermal boundary conditions.

Figure 7 shows the ratio of $\overline{Nu}_D/\overline{Nu}_{D,f}$ plotted against the buoyancy parameter κ^* . The scatter of points is due to the choice of the exponent n in the mixed convection parameter. In other words, there is no unique value of the exponent n in the parameter $Gr_D^*/(Re_D)^n$ that would fit all experimental data. The scatter of points was also noted by Sharma and Sukhatme.¹⁴

The experimental data from the present study for the mixed convection heat transfer is correlated (using the least-squares method) as

$$\overline{Nu}_D/\overline{Nu}_{D,f} = 1.009 + 0.0984\kappa^* - 0.0277(\kappa^*)^2 + 0.0032(\kappa^*)^3 \quad (7a)$$

where $\overline{Nu}_{D,f}$ is given in Eq. (5), and where

$$0 \leq [\kappa^* \equiv Gr_D^*/(Re_D)^{1.8}] \leq 4.6 \quad (7b)$$

In the limiting case ($\kappa^* = 0$), the proposed correlation [Eq. (7a)] overestimates the Nusselt number in forced convection by less than 1%.

Boundary Between Forced and Mixed Convection Regimes

The selection of the exponent 1.8 in the definition of κ^* [Eq. (7b)] was justified from the boundary points between forced and mixed convection regimes, where the ratio of $\overline{Nu}_D/\overline{Nu}_{D,f} \approx 1.05$. At a maximum value of $\kappa^* = 4.6$, the maximum increase in the Nusselt number due to the buoyancy effects is as much as 20%. If forced convection is assumed to exist, when \overline{Nu}_D is within 5% of $\overline{Nu}_{D,f}$, and by setting the left side of Eq. (7a) to 1.05 and solving the cubic equation for κ^* yields a value for $\kappa^* = 0.6$. Thus, the forced convection regime exists when $\kappa^* < 0.60$.

The transition point between mixed and free-convection regimes was not achieved in these tests due to lower speed limit on the fan motor which goes a minimum velocity of 1.4 m/s. In addition, the maximum heat flux supplied to the fiber

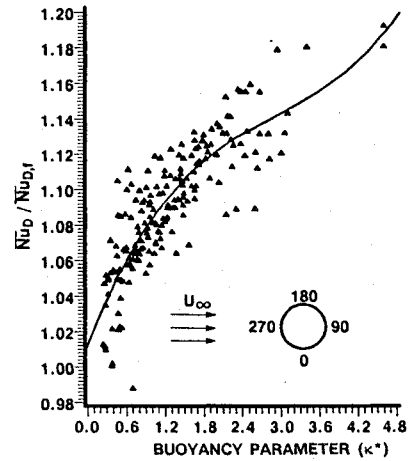


Fig. 7 Correlation of Nusselt number in terms of the derived buoyancy parameter.

cylinder (5000 W/m^2) was the upper limit on heat flux that the cylinder could endure before it will be mechanically distorted.

Summary and Conclusions

Buoyancy effects on forced convection from a uniform heat flux horizontal cylinder in a crossflow have been studied experimentally.

The following statements summarize the results of this experiment and the conclusions that were reached:

1) Convective heat transfer results are highly dependent on flow conditions. Flowfield quality and good use of the wind tunnel is as important as the intricacy and accuracy needed in the design of the test specimen.

2) The local Nusselt number around the cylinder in the mixed convection regimes as a function of the Reynolds and modified Grashof numbers is presented. The distortion of an otherwise symmetrical Nusselt number due to buoyancy has been shown.

3) The average Nusselt number in the mixed convection regime was correlated in the present study in comparison with the average forced convection Nusselt number ($\overline{Nu}_D/\overline{Nu}_{D,f}$) as a function of the buoyancy parameter (κ^*), and compared with other correlations found in literature.

4) The average Nusselt number around the cylinder in the forced convection regimes is presented as a limiting case. This condition was achieved when the ratio $1.0 \leq \overline{Nu}_D/\overline{Nu}_{D,f} < 1.05$.

5) In the forced convection regime it was found that a uniform heat flux cylinder (present study) has a higher Nusselt number than the same cylinder under a uniform surface temperature boundary condition.

6) Heat transfer in the mixed convection regime increased above the values that would exist in purely forced convection. A maximum increase in the Nusselt number due to free convection was found to be as much as 20%.

7) A predictive parameter and its value to define the boundary between forced and mixed convection regimes have been established. The forced convection regime was found to exist for $\kappa^* < 0.60$ based on present results.

Acknowledgments

This study was supported by the National Science Foundation under Grant MEA-8204361 and the University of Illinois Research Board. The authors express their appreciation to W. Ross, G. Sliva, F. Butzbacher, and H. Nurnberg for their valuable suggestions in building the experimental apparatus.

References

- 1) Van Der Hegge Zijnen, B. G., "Modified Correlation Formulae for Heat Transfers by Natural and by Forced Convection from Hor-

- izontal Cylinders," *Applied Scientific Research*, Vol. 6, Sec. A, 1956, pp. 129–140.
- ²Collis, D. C., and Williams, M. J., "Two-Dimensional Convection from Heated Wires at Low Reynolds Number," *Journal of Fluid Mechanics*, Vol. 6, Pt. 3, Oct. 1959, pp. 357–384.
- ³Sparrow, E. M., and Lee, L., "Analysis of Mixed Convection About a Horizontal Cylinder," *International Journal of Heat and Mass Transfer*, Vol. 19, No. 2, 1976, pp. 229–232.
- ⁴Joshi, N. D., and Sukhatme, S. P., "An Analysis of Combined Free and Forced Convection Heat Transfer from a Horizontal Circular Cylinder to a Transverse Flow," *Journal of Heat Transfer*, Vol. 93, Ser. C, No. 4, 1971, pp. 441–448.
- ⁵Merkin, J. H., "Mixed Convection from a Horizontal Circular Cylinder," *International Journal of Heat and Mass Transfer*, Vol. 20, No. 1, 1977, pp. 73–77.
- ⁶Jain, P. C., and Lohar, B. L., "Unsteady Mixed Convection Heat Transfer from a Horizontal Circular Cylinder," *Journal of Heat Transfer*, Vol. 101, Ser. C, No. 1, 1979, pp. 126–131.
- ⁷Nakai, S., and Okazaki, T., "Heat Transfer from a Horizontal Circular Wire at Small Reynolds and Grashof Numbers—II," *International Journal of Heat and Mass Transfer*, Vol. 18, No. 3, 1975, pp. 397–413.
- ⁸Badr, H. M., "A Theoretical Study of Laminar Mixed Convection from a Horizontal Cylinder in a Cross Stream," *International Journal of Heat and Mass Transfer*, Vol. 26, No. 5, 1983, pp. 639–653.
- ⁹Hatton, A. P., James, D. D., and Swire, H. W., "Combined Forced and Natural Convection with Low-Speed Air Flow over Horizontal Cylinders," *Journal of Fluid Mechanics*, Vol. 42, Pt. 1, June 1970, pp. 17–31.
- ¹⁰Oosthuizen, P. H., and Madan, S., "Combined Convective Heat Transfer from Horizontal Cylinders in Air," *Journal of Heat Transfer*, Vol. 92, Ser. C, No. 1, 1970, pp. 194–196.
- ¹¹Jackson, T. W., and Yen, H. H., "Combined Forced and Free Convective Equations to Represent Combined Heat-Transfer Coefficients for a Horizontal Cylinder," *Journal of Heat Transfer*, Vol. 93, Ser. C, No. 2, 1971, pp. 247, 248.
- ¹²Oosthuizen, P. H., and Madan, S., "The Effect of Flow Direction on Combined Convective Heat Transfer from Cylinders to Air," *Journal of Heat Transfer*, Vol. 93, Ser. C, No. 2, 1971, pp. 240–242.
- ¹³Ahmad, R. A., and Qureshi, Z. H., "Laminar Mixed Convection from a Uniform Heat Flux Cylinder," *Journal of Thermophysics and Heat Transfer*, Vol. 6, No. 2, 1992, pp. 277–287.
- ¹⁴Sharma, G. K., and Sukhatme, S. P., "Combined Free and Forced Convection Heat Transfer from a Heated Tube to a Transverse Air Stream," *Journal of Heat Transfer*, Vol. 91, Ser. C, No. 3, 1969, pp. 457–459.
- ¹⁵Gebhart, B., and Pera, L., "Mixed Convection from Long Horizontal Cylinders," *Journal of Fluid Mechanics*, Vol. 45, Pt. 1, Jan. 1971, pp. 49–64.
- ¹⁶Nayak, S. K., and Sandborn, V. A., "Periodic Heat Transfer in Directly Opposed Free and Forced Convection Flow," *International Journal of Heat and Mass Transfer*, Vol. 20, No. 3, 1977, pp. 189–194.
- ¹⁷Fand, R. M., and Keswani, K. K., "Combined Natural and Forced Convection Heat Transfer from Horizontal Cylinders to Water," *International Journal of Heat and Mass Transfer*, Vol. 16, No. 6, 1973, pp. 1175–1191.
- ¹⁸Krall, K. M., and Eckert, E. R. G., "Local Heat Transfer Around a Cylinder at Low Reynolds Number," *Journal of Heat Transfer*, Vol. 95, Ser. C, No. 2, 1973, pp. 273–275.
- ¹⁹Sarma, T. S., and Sukhatme, S. P., "Local Heat Transfer from a Horizontal Cylinder to Air in Cross Flow: Influence of Free Convection and Free Stream Turbulence," *International Journal of Heat and Mass Transfer*, Vol. 20, No. 1, 1977, pp. 51–56.
- ²⁰Morgan, V. T., "The Overall Convective Heat Transfer from Smooth Circular Cylinder," *Advances in Heat Transfer*, edited by T. F. Irvine, Jr., and J. P. Hartnett, Vol. 11, Academic Press, New York, 1975, pp. 199–264.
- ²¹Baughn, J. W., "Effect of Circumferential Wall Heat Conduction on Boundary Conditions for Heat Transfer in a Circular Tube," *Journal of Heat Transfer*, Vol. 100, Ser. C, No. 3, 1978, pp. 537–539.
- ²²Seban, R. A., "Heat Transfer to the Turbulent Separated Flow of Air Downstream of a Step in the Surface of a Plate," *Journal of Heat Transfer*, Vol. 86, Ser. C, No. 2, 1964, pp. 259–264.
- ²³Giedt, W. H., "Investigation of Variations of Point Unit Heat-Transfer Coefficient Around a Cylinder Normal to an Air Stream," *Transactions of the American Society of Mechanical Engineers*, Vol. 71, No. 4, 1949, pp. 375–381.
- ²⁴Petrie, A. M., and Simpson, H. C., "An Experimental Study of the Sensitivity to Freestream Turbulence of Heat Transfer Wakes of Cylinders in Crossflow," *International Journal of Heat and Mass Transfer*, Vol. 15, No. 8, 1972, pp. 1497–1513.
- ²⁵Hatton, A. P., and Woolley, N. H., "Heated Transfer in Two-Dimensional Turbulent Confined Flows," *Proceedings of the Institution of Mechanical Engineers*, Vol. 186, No. 53, 1972, pp. 625–633.
- ²⁶Simonich, J. C., and Moffat, R. J., "New Technique for Mapping Heat-Transfer Coefficient Contours," *Review of Scientific Instruments*, Vol. 53, No. 5, 1982, pp. 678–683.
- ²⁷Hippensteele, S. A., Russel, L. M., and Stepka, F. S., "Evaluation of a Method for Heat Transfer Measurements and Thermal Visualization Using a Composite of a Heater Element and Liquid Crystals," *Journal of Heat Transfer*, Vol. 105, No. 1, 1983, pp. 184–189.
- ²⁸Baughn, J. W., Takahashi, R. K., Hoffman, M. A., and McKillop, A. A., "Local Heat Transfer Measurements Using an Electrically Heated Thin Gold-Coated Plastic Sheet," *Journal of Heat Transfer*, Vol. 107, No. 4, 1985, pp. 953–959.
- ²⁹Baughn, J. W., Elderkin, M. J., and McKillop, A. A., "Heat Transfer from a Single Cylinder, Cylinders in Tandem, and Cylinders in the Entrance Region of a Tube Bank with a Uniform Heat Flux," *Journal of Heat Transfer*, Vol. 108, No. 2, 1986, pp. 386–391.
- ³⁰Ahmad, R. A., "Mixed Convection Around a Horizontal Cylinder," Ph.D. Dissertation, Univ. of Illinois, Chicago, IL, March 1985.
- ³¹Ahmad, R. A., and Qureshi, Z. H., "Buoyancy Effects on Forced Convection from a Uniform Heat Flux Cylinder," AIAA 30th Aerospace Sciences Meeting and Exhibit, AIAA Paper 92-0711, Reno, NV, Jan. 6–9, 1992.
- ³²Kestin, J., "The Effect of Free-Stream Turbulence on Heat Transfer Rates," *Advances in Heat Transfer*, edited by T. F. Irvine, Jr., and J. P. Hartnett, Vol. 3, Academic Press, New York, 1966, pp. 1–32.
- ³³Schlichting, H., *Boundary Layer Theory*, 7th ed., McGraw-Hill, New York, 1979, Chap. 12, p. 305.
- ³⁴Lowery, G. W., and Vachon, R. I., "The Effects of Turbulence on Heat Transfer from Heated Cylinders," *International Journal of Heat and Mass Transfer*, Vol. 18, No. 11, 1975, pp. 1229–1242.
- ³⁵Sikmanovic, S., Oka, S., and Koncar-Djurdjevic, S., "Influence of the Structure of Turbulent Flow on Heat Transfer from a Single Cylinder in a Crossflow," *Proceedings of the Fifth International Heat Transfer Conference*, Hemisphere, Tokyo, Vol. 2, Sept. 3–7, 1974, FC 8.6, pp. 320–324.
- ³⁶Dyban, E. P., and Epick, E. Y., "Some Heat Transfer Features in the Airflows of Intensified Turbulence," *Proceedings of the Fourth International Heat Transfer Conference*, Paris and Versailles, France, edited by U. Grigull, and E. Hahne, Elsevier, Amsterdam, The Netherlands, FC 5.7, 1970.
- ³⁷Baughn, J. W., Ireland, P. T., Jones, T. V., and Saniei, N., "A Comparison of the Transient and Heated-Coating Methods for the Measurements of Local Heat Transfer Coefficients on a Pin Fin," *Journal of Heat Transfer*, Vol. 111, No. 4, 1989, pp. 877–881.
- ³⁸Van Der Hegge Zijnen, B. G., "Heat Transfer from Horizontal Cylinders to a Turbulent Flow," *Applied Scientific Research*, Vol. 7, Sec. A, 1958, pp. 205–223.
- ³⁹Achenbach, E., "Total and Local Heat Transfer from a Smooth Circular Cylinder in Cross-Flow at High Reynolds Number," *International Journal of Heat and Mass Transfer*, Vol. 18, No. 12, 1975, pp. 1387–1396.
- ⁴⁰Qureshi, Z. H., and Ahmad, R. A., "Natural Convection from a Horizontal Cylinder at Moderate Rayleigh Numbers," *Numerical Heat Transfer*, Vol. 11, No. 2, 1987, pp. 199–212.
- ⁴¹Kays, W. M., and Crawford, M. E., *Convective Heat and Mass Transfer*, 2nd ed., McGraw-Hill, New York, 1980, Chap. 9.
- ⁴²Churchill, S. W., and Chu, H. H. S., "Correlating Equations for Laminar and Turbulent Free Convection from a Vertical Plate," *International Journal of Heat and Mass Transfer*, Vol. 18, No. 11, 1975, pp. 1323–1329.
- ⁴³Baughn, J. W., and Saniei, N., "The Effect of the Thermal Boundary Condition on Heat Transfer from a Cylinder in Crossflow," *Journal of Heat Transfer*, Vol. 113, No. 4, 1991, pp. 1020–1023.
- ⁴⁴Papell, S. S., "Influence of Thermal Boundary Conditions on Heat Transfer from a Cylinder in Crossflow," NASA TP 1894, Lewis Research Center, Aug. 1981 (eight unnumbered pages).
- ⁴⁵O'Brien, J. E., Simoneau, R. J., LaGraff, J. E., and Morehouse, K. A., "Unsteady Heat Transfer and Direct Comparison for Steady-State Measurements in a Rotor-Wake Experiment," *Proceedings of the Eighth International Heat Transfer Conference*, San Francisco, CA, Aug. 1986, edited by C. L. Tien, V. P. Carey, and J. K. Ferrell, Hemisphere, New York, pp. 1243–1248.